Optics Communications 383 (2017) 255–259

Contents lists available at ScienceDirect

Optics Communications

journal homepage: www.elsevier.com/locate/optcom

Investigation of inhomogeneity and anisotropy in near ground layers of atmospheric air turbulence using image motion monitoring method

Ebrahim Mohammadi Razi [a,b,*], Saifollah Rasouli [b,c]

[a] Department of Physics, Faculty of Basic Science, University of Bojnord, P.O. Box: 1339, Bojnord, Iran
[b] Department of Physics, Institute of Advanced Studies in Basic Sciences, P.O. Box: 45195-1159, Zanjan, Iran
[c] Optics Research Center, Institute for Advanced Studies in Basic Sciences, P.O. Box: 45195-1159, Zanjan, Iran

ARTICLE INFO

Article history:
Received 12 July 2016
Received in revised form
11 August 2016
Accepted 30 August 2016

Keywords:
Atmospheric turbulence
Light propagation
Signal processing
Image motion monitoring

ABSTRACT

In this work the anisotropy and inhomogeneity of real atmospheric turbulence have been investigated using image motion monitoring and differential image motion monitoring methods. For this purpose the light beam of a point source is propagated through the atmospheric turbulence layers in horizontal path and then impinged to a telescope aperture. The telescope and point source were 350 m apart. In front of the telescope's aperture a mask consisting of four subapertures was installed. Image of the point source was formed on a sensitive CCD camera located at the focal plane of the telescope. By displacing CCD camera along the axis of telescope, four distinct images were recorded. Angle of arrival (AA) of each spot was calculated by image processing. Air turbulence causes AA to fluctuate. By comparing AA fluctuation variances of different spots in two directions isotropy and homogeneity of turbulence were studied. Results have shown that atmospheric turbulence in near ground layers is treated as an anisotropic and inhomogeneous medium. In addition, the inhomogeneity and anisotropy of turbulence decreases with the distance from earth surface.

© 2016 Elsevier B.V. All rights reserved.

1. Introduction

Studying atmospheric turbulence is important due to its role in optical remote sensing and communication. All the models being presented for studying turbulence especially atmospheric turbulence are based on homogeneity and isotropy of turbulence in inertial range [1]. The Kolmogorov model is the most common one. The isotropy and homogeneity of the atmospheric turbulence are almost valid for a light beam propagating in vertical path, while for a light beam propagating in horizontal path these hypotheses are not valid, especially in near ground layers of atmospheric turbulence [2–6]. It seems that, deviation of atmospheric turbulence behavior from Kolmogorov model is due to the assumptions of homogeneity and isotropy of turbulence that this model was based on. Various optical methods are used to study atmospheric turbulence characteristics, namely methods based on “wave front sensor” [7,8], “shearing interferometry” [9], “curvature sensor” [10], “moire' based deflectometry” [11–15], and “image motion monitoring” using an optical system with multi-apertures [16–20]. Among these, image motion monitoring is commonly used due to its simple setup as well as simple analyzing data. This method was been used for characterization of atmospheric turbulence since early 20th century. For the first time Schlesinger used star trials for measuring atmospheric seeing [21]. Using Tatarski's model for wave propagation through the atmosphere, Fried derived the rms of image motion [22]. In the mentioned researches, results may be biased with an error due to the telescope vibrations contributing image motion. To solve this problem, Stock and Keller introduced the concept of differential image motion monitoring (DIMM) [23]. In this approach a mask with two similar apertures is installed in front of the entrance pupil of telescope. The two apertures create two images from single star in the focal plane of telescope. By measuring the relative motion of the two images, optical parameters of atmospheric turbulence can be calculated. Sarazin and Roddier [24] and Vernin and Munoz-Tunon [20] and Tokovinin [18] developed the modern implementation of DIMM. Using differential image motion monitoring results in removing similar fluctuations of two images and therefore the telescope vibration effect does not appear in the results. After developing the 2-apertures DIMM, Shomali et al. [25] produced a 4-aperture differential image motion monitoring method to measure the atmospheric primary aberrations. In this work, we investigate the homogeneity and isotropy of atmospheric turbulence at near ground layers by non-differential and differential image motion monitoring methods using a similar

* Corresponding author at: Department of Physics, Faculty of Basic Science, University of Bojnord, P.O. Box: 1339, Bojnord, Iran.
E-mail address: e.mohammadi@ub.ac.ir (E. Mohammadi Razi).

http://dx.doi.org/10.1016/j.optcom.2016.08.080
0030-4018/© 2016 Elsevier B.V. All rights reserved.

setup of 4-DIMM: light beam propagates in horizontal path through atmospheric turbulence and then incident to an optical system with four interence apertures. Recently, we have published a paper on homogeneity and isotropy of convective air turbulence investigating by non-differential image motion monitoring method with 4 apertures optical system [26]. In that work, we used two telescopes face to face to generate, propagate and receive plane waves. Plane waves emerging from the first telescope passed through turbulent medium, then the deformed wavefront entered into the second telescope. A flat plane heater was used to produce vertical temperature gradient and consequently indoor convective air turbulence. A mask consisting of four apertures is installed in the interence pupil of second telescope. Four distinct images were recorded by a CCD camera installed in out-of-focus plane of second telescope. By measuring local AA fluctuations of aberrated wavefront at region of four apertures and then calculating variances of these fluctuations in two directions, homogeneity and isotropy of convective air turbulence were studied. The results showed that the laboratory convective air turbulence is an anisotropic and inhomogeneous medium. In this work, a similar procedure of studying statistical fluctuation of images motion was used to investigate homogeneity and isotropy of atmospheric turbulence.

2. Experiment

Fig. 1 shows the schematic diagram of experimental setup used in IASBS campus at Zanjan on July 26, 2012. According to the figure, a white light point source was installed at a height of 60 cm from earth surface. Light beam of the point source propagates through the atmospheric turbulence in a horizontal path and impinges on the aperture of a telescope. The telescope and point source were 350 m apart. The telescope (Meade 8 in LX200 GPS Schmidt-Cassegrain telescope) has a diameter of 20.13 cm and focal length of 200 cm. A mask consisting of four widely separated small subapertures was installed in front of telescope's aperture. Adjacent subapertures are 10.16 cm apart and had a diameter of 3 cm (Fig. 2). Image of a point source is formed on a sensitive CCD camera (DCC1545Mhigh resolution USB2.0 CMOS Camera, Monochrome) located at the focal plane of the telescope. By displacing CCD along the axis of telescope, four distinct images were recorded. Frame rate of image recording and exposure time were set to 60 frame/s and 8 and 16 ms, respectively. Fig. 2 shows the geometry of the four subapertures and a typical image recorded by the CCD located in out of focus plane. To reduce background noise, all the experiments have been carried out at night. The experiment was repeated 6 times with an interval of 2 min. During all the experiments, weather condition was calm and almost the same. Each data consisting of 5000 images were taken at about 83 s.

3. Data analyses

Calculation method of AA has been fully described in Ref. [26]. In summary AA of the light beam in x-direction can be calculated as follows:

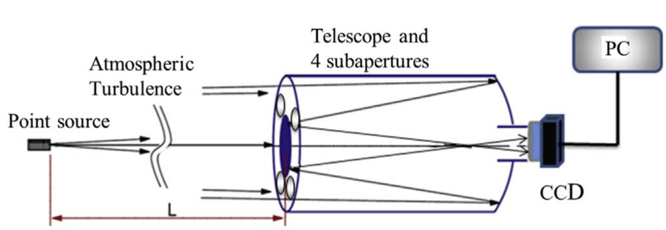

Fig. 1. (color online) Schematic diagram of experimental setup, L=350 m.

$$\alpha_{xi} = \frac{l_x\left(x_{gi} - \bar{x}_{gi}\right)}{f}, \quad i = 1, 2, 3, 4, \tag{1}$$

where l_x, x_{gi}, $\bar{x}_{gi}$ and f are the pixel size in the x-direction on the image plane, x component of center of the image of ith subaperture, the mean position of center of the image in x-direction, and the telescope focal length, respectively. AA of the incident beam in subaperture's locations is fluctuated due to atmospheric turbulence. Fig. 3 shows the typical time series of AA fluctuations in two directions, parallel to the earth surface and perpendicular to it, when the exposure time of CCD camera was set to 8 ms.

As said, to record 4 distinct images, CCD camera was installed in out of focus plane of the telescope. In the experiment, focal length of telescope was 200 cm and CCD camera was located 3 mm outside of the focal plane of the telescope. In AA calculation, the value of the focal length of the telescope was set equal to 200.3 cm [26]. Since the CCD camera was located slightly out-of-focus, the wavefront aberration of light beam causes error in determining the centroid of each spots. To get rid of this problem, the frames with Strehl ratio of any spots smaller than 0.6 were rejected. The Strehl ratio, S, can be estimated as [18]

$$S = \frac{I_{max}}{I_{total}}\frac{4}{\pi}\left(\frac{\lambda_{CCD}}{D\Delta x}\right), \tag{2}$$

where I_{max}, I_{total}, Δx, λ_{CCD} and D are the maximum pixel intensity in a spot, total flux (sum over the pixels), pixel size in radians, the maximum CCD sensitivity and apertures diameter, respectively.

To investigate of homogeneity and isotropy of atmospheric turbulence we calculated the variance of AA fluctuations in two directions for all spots. The related results for all spots with exposure time of 8 and 16 ms are presented in Table 1.

The average value of variances of x and y components of AA fluctuations for 8 ms exposure time are as follows:

$$\begin{aligned}
&\bar{\sigma}^2_{\alpha x1} = 4.79 \times 10^{-11}\,\text{rad}^2, \quad \bar{\sigma}^2_{\alpha y1} = 9.16 \times 10^{-11}\,\text{rad}^2,\\
&\bar{\sigma}^2_{\alpha x2} = 4.59 \times 10^{-11}\,\text{rad}^2, \quad \bar{\sigma}^2_{\alpha y2} = 9.15 \times 10^{-11}\,\text{rad}^2,\\
&\bar{\sigma}^2_{\alpha x3} = 4.78 \times 10^{-11}\,\text{rad}^2, \quad \bar{\sigma}^2_{\alpha y3} = 10.74 \times 10^{-11}\,\text{rad}^2,\\
&\bar{\sigma}^2_{\alpha x4} = 5.03 \times 10^{-11}\,\text{rad}^2, \quad \bar{\sigma}^2_{\alpha y4} = 10.12 \times 10^{-11}\,\text{rad}^2,
\end{aligned} \tag{3}$$

where $\bar{\sigma}^2_{\alpha xi}$ and $\bar{\sigma}^2_{\alpha yi}$ are the mean value of AA fluctuations variances of ith aperture in x-direction and y-direction, respectively. Similarly, the mean value of AA fluctuations variances for 16 ms exposure time are

$$\begin{aligned}
&\bar{\sigma}^2_{\alpha x1} = 3.66 \times 10^{-11}\,\text{rad}^2, \quad \bar{\sigma}^2_{\alpha y1} = 7.06 \times 10^{-11}\,\text{rad}^2,\\
&\bar{\sigma}^2_{\alpha x2} = 3.44 \times 10^{-11}\,\text{rad}^2, \quad \bar{\sigma}^2_{\alpha y2} = 6.57 \times 10^{-11}\,\text{rad}^2,\\
&\bar{\sigma}^2_{\alpha x3} = 4.19 \times 10^{-11}\,\text{rad}^2, \quad \bar{\sigma}^2_{\alpha y3} = 7.95 \times 10^{-11}\,\text{rad}^2,\\
&\bar{\sigma}^2_{\alpha x4} = 3.72 \times 10^{-11}\,\text{rad}^2, \quad \bar{\sigma}^2_{\alpha y4} = 7.8 \times 10^{-11}\,\text{rad}^2,
\end{aligned} \tag{4}$$

According to the results, increasing the exposure frame time reduces the variances of AA fluctuations. This is because, in long exposure time some fluctuations are removed due to averaging thus the variance is reduced. In addition in all cases variances of AA fluctuations in two directions are not equal namely, $\sigma^2_{\alpha xi} < \sigma^2_{\alpha yi}$. In other words, the atmospheric turbulence in near ground layers is anisotropic. further more, since $\sigma^2_{\alpha x1} \neq \sigma^2_{\alpha x2}$ and $\sigma^2_{\alpha x3} \neq \sigma^2_{\alpha x4}$ the turbulence is inhomogeneous in x-direction. This result is established for (1,3) and (2,4) pair apertures as well. We came to the same conclusion on anisotropy and inhomogeneity of indoor convective air turbulence [26]. For further discussion, we introduce the anisotropy coefficient for the pair of upper and lower apertures:

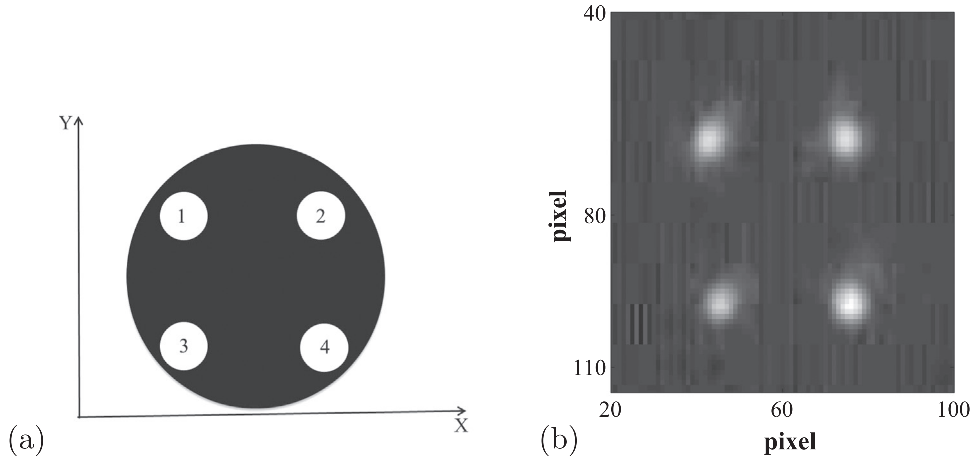

Fig. 2. (a) Geometry of the subapertures on the telescope's pupil and (b) a typical recorded frame in out of focus plane of telescope.

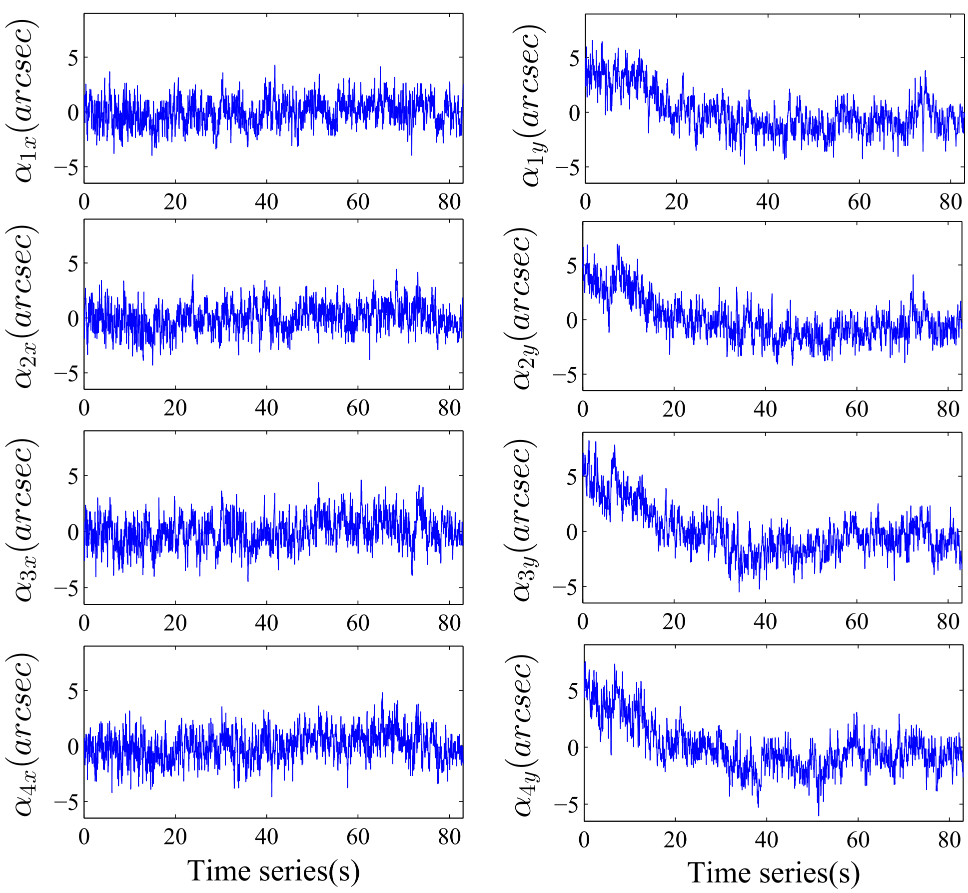

Fig. 3. Vertical and horizontal components (y and x directions, respectively) of the AA fluctuations over four subapertures on the telescope pupil versus the time. The exposure time was set to 8 ms.

Table 1
Variance of AA fluctuations of spot's image $\left(\times 10^{-11}\,\mathrm{rad}^2\right)$.

Exposure time	$\sigma^2_{\alpha x1}$	$\sigma^2_{\alpha y1}$	$\sigma^2_{\alpha x2}$	$\sigma^2_{\alpha y2}$	$\sigma^2_{\alpha x3}$	$\sigma^2_{\alpha y3}$	$\sigma^2_{\alpha x4}$	$\sigma^2_{\alpha y4}$
8 ms	4.038	4.503	3.476	4.347	3.770	4.819	3.778	5.014
	4.302	7.885	4.157	7.731	4.233	9.830	4.821	9.733
	6.04	15.12	6.14	15.38	6.36	17.59	6.51	15.29
16 ms	3.885	8.547	3.602	7.673	4.315	8.102	3.973	8.516
	3.686	3.907	3.449	3.569	4.155	4.440	3.275	4.401
	3.430	8.740	3.290	8.480	4.110	11.32	3.92	10.58

$$\gamma = \frac{\frac{\sigma_{yi}^2 + \sigma_{yj}^2}{2}}{\frac{\sigma_{xi}^2 + \sigma_{xj}^2}{2}} = \begin{cases} \dfrac{9.155 \times 10^{-11}}{4.69 \times 10^{-11}} = 1.95 & \text{for } (i, j = 1, 2), \\ \dfrac{10.43 \times 10^{-11}}{4.90 \times 10^{-11}} = 2.12 & \text{for } (i, j = 3, 4), \end{cases} \tag{5}$$

where $\sigma^2_{\alpha xi}$ and $\sigma^2_{\alpha yj}$ are variance of AA fluctuations in x-direction for ith subaperture and variance of AA fluctuations in y-direction for jth subaperture, respectively. The error in the calculated anisotropy coefficient is estimated to be $\frac{\delta\gamma}{\gamma} = 0.04$. According to Eq. (5), the variances of AA fluctuations and turbulence intensity are stronger in lower apertures due to the enhanced temperature gradients. Addition anisotropy coefficient increases as height from earth surface decreases. A similar result has been found out for indoor convective air turbulence. In other words, anisotropy increases due to increasing of temperature gradient. The theoretical study of this claim is the subject that we keep in mind to do in future. In addition, in Refs. [2–4] Lukin et al. in similar approach found same results in study of anisotropy of atmospheric turbulence at altitude of 1.5 m above the ground surface by taking into account of the outer scale effects. It should be noted that for competent assessment of anisotropy necessary measure wind speed as a vector, i.e., its vertical and horizontal components are needed which unfortunately has not been done in these trials.

Similarly, one can produce inhomogeneity coefficient for different height as follows:

$$\beta = \frac{\sigma_{xi}^2 - \sigma_{xj}^2}{\frac{\sigma_{xi}^2 + \sigma_{xj}^2}{2}} \times 100 = \begin{cases} 4.26\% & \text{for } (i, j = 1, 2), \\ 5.1\% & \text{for } (i, j = 3, 4). \end{cases} \tag{6}$$

The maximum estimated error in inhomogeneity coefficient is $\frac{\delta\beta}{\beta} = 0.5$. According to Eq. (6), inhomogeneity of atmospheric turbulence increases as distance from the ground decreases. We know that the different parts of Earth surface absorb different amount of solar energy and consequently have different temperatures. This creates different temperature gradients along the Earth surface. Perpendicular to the Earth surface different temperature gradients appear. Thus due to the Earth surface profile and the existence of no constant and no equal temperature gradients in the vertical and horizontal directions at various altitudes and locations, it is reasonable to expect that for a light beam propagating through atmospheric turbulence especially near the Earth surface on a horizontal path, the homogeneity and isotropy of the atmospheric turbulence as shown be violated.

As mentioned above, the results of this work are in complete agreement with our experiment on the convective air turbulence. It should be emphasized that due to not using the differential image motion monitoring method (DIMM), results may be biased owing to telescope vibration in presence of wind flow and earth vibrations. The longitudinal and transverse component of AA fluctuations cross correlation for pair image of (1, 2), i.e. along and perpendicular to the connecting line of the apertures, respectively, are shown in Fig. 4 to check the vibrations effect. According to the figure there is a significant transverse cross correlation of AA fluctuations for pair of (1, 2) spots during long time, in contrast to the longitudinal component. This significant long time cross correlation may be associated to the telescope vibrations. Thus AA fluctuations variances in y direction may be biased by telescope vibrations. To remove the unwanted vibration effects, the differential image motion monitoring method (DIMM) was used [18]. In this method we can calculate the atmospheric seeing by measuring variance of differential of AA fluctuations of two images in two directions, as follows:

$$\sigma_{l(t)}^2 = K_{l(t)}\lambda^2 r_{0l(t)}^{-5/3} D^{-1/3}, \tag{7}$$

where σ^2, r_0, λ and D are variance of differential image motion, Fried parameter, wavelength and diameter of each apertures, respectively. The subscripts l and t refer to the longitudinal and transverse situations, respectively. In a DIMM, two circular portions of the wavefront are isolated. The variance of the differential wavefront tilts in longitudinal and transverse directions is related to the Fried parameter as Eq. (7). The response coefficients of DIMM K_l and K_t are related to the ratio of distance separation between apertures and apertures diameter ($b = \frac{B}{D}$) and on the kind of the tilt measured. Usually, the tilt is evaluated from the centroids of two images formed by the sub-apertures; in this case it corresponds to the wavefront gradient and can be approximated as follows [18]:

$$K_l = 0.364\left(1 - 0.532 b^{-1/3} - 0.024 b^{-7/3}\right),$$
$$K_t = 0.364\left(1 - 0.798 b^{-1/3} + 0.018 b^{-7/3}\right), \tag{8}$$

In this way, by removing the same fluctuations from two images, telescope vibration effects do not appear in the results. Fried parameter in a typical direction is calculated from the variance of differential AA fluctuations of two images along that direction, as follows:

$$\sigma_{x(y)}^2 = K\lambda^2 r_{0x(y)}^{-5/3} D^{-1/3} \Longrightarrow r_{0x(y)} = \left(\frac{K\lambda^2 D^{-1/3}}{\sigma_{x(y)}^2}\right)^{3/5}, \tag{9}$$

here, the statistical error of Fried parameter is calculated from [27]

$$\frac{\delta r_0}{r_0} = \sqrt{\left(\frac{\delta K}{K}\right)^2 + \left(\frac{\delta\lambda}{\lambda}\right)^2 + \left(\frac{\delta D}{D}\right)^2 + \left(\frac{\delta\sigma_{x(y)}^2}{\sigma_{x(y)}^2}\right)^2}, \tag{10}$$

considering $\frac{\delta K}{K} = 0.004$, $\frac{\delta D}{D} = 0.003$ pixel, $\delta\lambda$ is negligible, and $\frac{\delta\sigma_{x(y)}^2}{\sigma_{x(y)}^2} = 0.02$, value of $\frac{\delta r_0}{r_0} = 0.02$ is obtained. If atmospheric turbulence is isotropic one expects the longitudinal Fried parameter calculated from pair apertures (1,2) and (1,3) to be equal. According to the geometry of subapertures shown in Fig. 2, the average longitudinal Fried parameter calculated from pair subapertures are:

$$\bar{r}_{0l}(1,2) = 30.4\ \text{mm}, \quad \bar{r}_{0l}(3,4) = 29.06\ \text{mm},$$
$$\bar{r}_{0l}(1,3) = 28.96\ \text{mm}, \quad \bar{r}_{0l}(2,4) = 28.46\ \text{mm}, \tag{11}$$

since $\bar{r}_{0l}(1,2)$ and $\bar{r}_{0l}(3,4)$ are not equal, one can conclude that

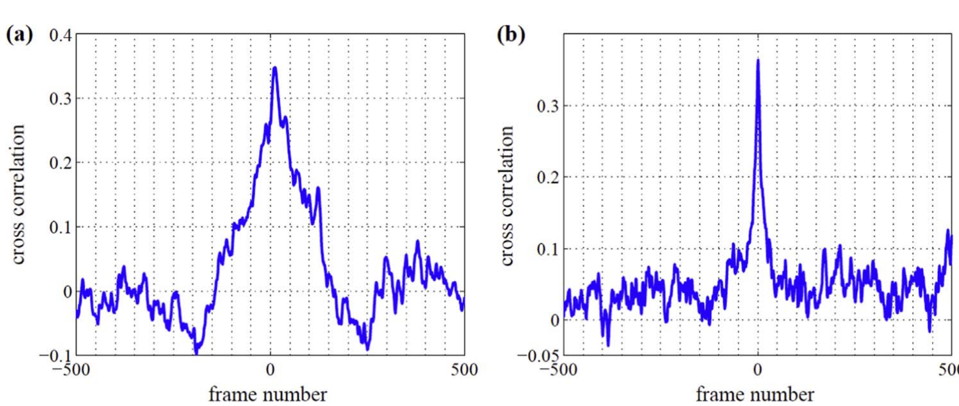

Fig. 4. (a) Transverse and (b) longitudinal component of cross correlation of AA fluctuations for spots of (1, 2).

atmospheric turbulence is inhomogeneous in y direction. Furthermore the anisotropy of atmospheric turbulence in height of $h + \frac{\Delta h}{2}$ (where h and Δh are height of apertures 3, 4 from the Earth surface and distance between apertures in $y(x)$ direction, respectively) is investigated by calculating $r_{0\parallel}$ and $r_{0\perp}$ as follows:

$$r_{0\parallel}\left(h + \frac{\Delta h}{2}\right) = \frac{r_{0l}(1, 2) + r_{0l}(3, 4)}{2} = \frac{30.4 + 29.06}{2} = 29.73 \text{ mm},$$
$$r_{0\perp}\left(h + \frac{\Delta h}{2}\right) = \frac{r_{0l}(1, 3) + r_{0l}(2, 4)}{2} = \frac{28.96 + 28.46}{2} = 28.71 \text{ mm}, \quad (12)$$

Since $r_{0\parallel}\left(h + \frac{\Delta h}{2}\right)$ and $r_{0\perp}\left(h + \frac{\Delta h}{2}\right)$ are not equal, atmospheric turbulence behavior is anisotropic at the height of $h + \frac{\Delta h}{2}$. As mentioned, using differential image motion monitoring method for calculating Fried parameter prohibits the effects of telescope vibrations from appearing in results.

4. Conclusion

Our recent investigation of indoor convective air turbulence in lab based on image motion monitoring method showed that it is an inhomogeneous and anisotropic medium [26]. Indoor convective air turbulence created by electrical heater was used to simulate the atmospheric turbulence especially in near ground layers in lab. In this work anisotropy and inhomogeneity of real atmospheric turbulence were investigated using two methods: image motion monitoring and differential image motion monitoring methods. Calculation of cross correlation of images showed that the results may be biased with telescope vibrations in image motion monitoring method. To remove the telescope vibration effects the differential image motion method was used. It was revealed from the results of two methods that the atmospheric turbulence in near ground layers is treated as an anisotropic and an inhomogeneous medium. In addition, anisotropy and inhomogeneity increase as the distance from surface decreases.

References

[1] L.C. Andrews, R.L. Phillips, Laser Beam Propagation Through Random Media, SPIE Press, Bellingham, Washington USA, 2005.
[2] V.P. Lukin, Investigation of some peculiarities in the structure of large scale atmospheric turbulence, in: Proceedings of the SPIE, vol. 2200, 199, pp. 384–395.
[3] V.P. Lukin, V. Pokasov, Appl. Opt. 20 (1981) 121.
[4] V.P. Lukin, Investigation of the anisotropy of the atmospheric turbulence spectrum in the low-frequency range, in: Proceedings of the SPIE, vol. 2471, 1995, pp. 347–355.
[5] I. Arad, B. Dhruva, S. Kurien, V.S. Lvov, I. Procaccia, K.R. Sreenivasan, Phys. Rev. Lett. 81 (1998) 5330.
[6] W. Du, L. Tan, J. Ma, S. Yu, Y. Jiang, Laser Part. Beams 28 (2010) 91.
[7] B.C. Platt, R. Shack, Refract. Surg. 17 (2001) 573.
[8] R.V. Shack, B.C. Platt, Opt. Soc. Am. 61 (1971) 656.
[9] G.W.R. Leibbrandt, G. Harbers, P.J. Kunst, Appl. Opt. 35 (1996) 6151.
[10] F. Roddier, Appl. Opt. 27 (1998) 1223.
[11] S. Rasouli, M.T. Tavassoly, Opt. Lett. 31 (2006) 3276.
[12] S. Rasouli, M.T. Tavassol, Opt. Lett. 33 (2008) 980.
[13] S. Rasouli, Opt. Lett. 35 (2010) 1470.
[14] S. Rasouli, M. Dashti, A.N. Ramaprakash, Opt. Express 18 (2010) 23906.
[15] M. Dashti, S. Rasouli, J. Opt. 14 (2012) 095704.
[16] D.L. Fried, Radio Sci. 10 (1975) 71.
[17] M. Sarazin, F. Roddier, Astron. Astrophys. 227 (1990) 294.
[18] A. Tokovinin, Publ. Astron. Soc. Pac. 114 (2002) 1156.
[19] J. Bally, D. Theil, Y. Billawala, D. Potter, R.F. Loewenstein, F. Mrozek, J.P. Lloyd, Publ. Astron. Soc. Aust. 13 (1996) 22.
[20] J. Vernin, C. Munoz-Tunon, Astron. Soc. Pac. 107 (1995) 265.
[21] F. Schlesinger, Pop. Astron. 21 (1913) 545.
[22] D.L. Fried, J. Opt. Soc. Am. 55 (1965) 1427.
[23] J. Stock, G. Keller, in: G.P. Kuiper, B.M. Middlehurst (Eds.), Telescopes, University of Chicago Press, Chicago, 1960, p. 151.
[24] M. Sarazin, F. Roddier, Astron. Astrophys. 227 (1990) 294.
[25] R. Shomali, S. Nasiri, A. Darudi, J. Opt. 13 (2011) 055708.
[26] E.M. Razi, S. Rasouli, J. Opt. 16 (2014) 045705.
[27] J.R. Taylor, An Introduction to Error Analysis the Study of Uncertainties in Physical Measurements, University Science Books, New York, 1997.